

Contents lists available at ScienceDirect

Journal of Catalysis

journal homepage: www.elsevier.com/locate/jcat



Enhancing both selectivity and activity of CO₂ conversion by breaking scaling relations with bimetallic active sites anchored in covalent organic frameworks



Lele Gong^a, Detao Zhang^a, Yang Shen^a, Xiaowei Wang^b, Jing Zhang^c, Xiao Han^c, Lipeng Zhang^{a,*}, Zhenhai Xia^{b,*}

- ^a College of Chemical Engineering, Beijing University of Chemical Technology, Beijing 100029, China
- ^b Department of Materials Science and Engineering, University of North Texas, Denton, TX 76203, USA
- ^c School of Materials Science and Engineering, Northwestern Polytechnical University, Xi'an 710072, China

ARTICLE INFO

Article history: Received 14 May 2020 Revised 23 June 2020 Accepted 23 July 2020 Available online 31 July 2020

Keywords:
Carbon dioxide reduction
Density functional theory calculation
Energy conversion
Bimetallic-atoms electrocatalysts
Design principles

ABSTRACT

The development of catalysts with high activity and selectivity for electrochemical reduction of CO₂ could provide renewable energy sources and improved environmental remediation. However, most current electrocatalysts have large energy barriers that lower their activity and selectivity. Here, we designed a class of electrocatalysts with 3d transition bimetallic active sites embedded into covalent organic frameworks (COFs) and discovered that they were more efficient than noble metals and single-atom electrocatalysts in CO₂ reduction reaction to CO. To facilitate rational design and quick screening of desired catalysts, an intrinsic descriptor was identified for the catalysts, which correlates the catalytic activity with the topological, bonding, and electronic structures. Among the catalysts, Fe/Cu-, Ni/Zn-COFs could be excellent electrocatalysts, with the low overpotential (~0.25 V) while suppressing side reactions. The excellent activity and selectivity of the catalysts stems from their unique bimetallic sites that break the constraint of scaling relations, leading to much more adsorption modes and facilitating intermediates to achieve the ideal states.

© 2020 Elsevier Inc. All rights reserved.

1. Introduction

The electrochemical reduction of carbon dioxide (CO₂) into carbon-neutral fuels provides a viable strategy to recycle and utilization of CO₂ in renewable energy conversion/storage and environmental remediation [1-5]. At the heart of CO_2 conversion technology, electrocatalysts are urgently needed to promote the critical reaction, namely CO₂ reduction reaction (CO₂RR). Recently, the single-atom catalysts (SACs) with high activity are emerging as one of the most promising candidates to replace the noble metals (Au, Ag) in CO₂ conversion [6-10]. The Fe-N-C and Co-N-C SACs have been demonstrated to be effective electrocatalysts for CO₂RR with high Faradaic efficiency [11-14]. However, there is often a large energy barrier in the elementary reaction of CO₂ chemisorption or product desorption, which increases their reactive overpotential and lowers their activity and selectivity [15,16]. These limitations are generally derived from the single-atomic centers that cannot simultaneously provide enough catalytic sites for

E-mail addresses: zhanglp@buct.edu.cn (L. Zhang), Zhenhai.xia@unt.edu (Z. Xia).

adsorbing and activating the chemically stable CO₂ molecules and their intermediates [17,18]. This result is supported by the first-principles calculation that if the CO₂ gas molecules are adsorbed on SACs with the C-terminal mode, one of the O atoms will be in an unstable state because the carbon–oxygen double bond is broken [19]. Despite a great progress in CO₂RR, therefore, there are still significant challenges in rationally designing an electrocatalyst with superior activity and selectivity for desirable products in CO₂RR.

The use of bimetals has been proven to be an effective way to improve the catalytic performance in numerous catalytic conversion reactions and seems to be expected to solve the above issues [20]. In nature, the biological enzymes with heterobinuclear centers (e.g., multinuclear Fe-Mo center in nitrogenases for nitrogen fixation) generally assume the task of highly efficient catalysis and are more active than the single ones for catalyzing complex reactions [21,22]. The bimetal design could even break the scaling effect due to their bi-active center and synergistic effect. Compared to the single-metal sites, the bimetal active sites are more favorable for providing more versatile electron transfer modes, orbitals, and geometric configurations to regulate adsorption or desorption

^{*} Corresponding authors.

of intermediates to satisfy the appropriate state to achieve higher catalytic activities [23–26]. Recently, Zhao [27] et al. have reported an iron-nickel (Fe/Ni) based bimetallic-atom electrocatalyst (BAC) that could significantly reduce the free energy of CO desorption into the gas phase and exhibited better catalytic performance for CO₂RR. Moreover, Li [28] et al. and Sun [29] et al. discovered two BACs, Fe/Co-BAC and Co/Zn-BAC, respectively, both of which have a better electrocatalytic performance for oxygen reduction reaction (ORR) than SACs. In addition to CO₂RR, the catalytic performance of BACs is also superior to SACs in many other reactions such as water splitting, nitrogen reduction, and CO oxidation [30–33]. Thence, it is of significance to experimentally and/or computationally explore the design principles for BACs, especially for complex chemical reactions such as CO₂RR.

Herein, we designed and proposed an exciting class of BACs, in which the sites of two transition metallic atoms are anchored by nitrogen atoms to form numerous "M₁/M₂-N₆" catalytic units in covalent organic frameworks (COFs). We aimed to understand CO₂-RR catalytic mechanism and provide design principles for experimental synthesis of these BACs. The density functional theory (DFT) calculations have then been utilized as reliable, efficient mainstream methods to quickly screen for catalysts with desirable catalytic performance [34,35]. A few descriptors have been discovered for describing the catalytic behaviors of different material systems including metal oxides, carbon nanomaterials and SACs [36– 41], but there lacks the inherent descriptors or design principles for the screening of the best catalysts from numerous BACs. In this work, the possible intermediates, free energy, reaction pathways and overpotential (η) of CO_2RR were considered and calculated with the DFT methods to identify the dominant products and explain the catalytic mechanism in depth. A new descriptor has been discovered that governs the catalytic activity of BCAs for CO₂-RR. This work thus provides a theoretical base for developing novel BACs in this thriving field of electrocatalysis.

2. Results

2.1. Molecular structures and stability of BAC-COFs

A series of BAC-based COFs (BAC-COFs) structures with two 3d transition metallic atoms in the center of " M_1/M_2 - N_6 " catalytic units (M_1 and M_2 = Sc, Ti, V, Cr, Mn, Fe, Co, Ni, Cu, and Zn) are created to study their CO₂RR catalytic activities (Fig. 1a). With COF substrates, these catalysts have high BET surface, porous structure, well-defined coordination structure and clear catalytic units, which provide large catalytic sites, promote the diffusion of gas molecules and facilitate the improvement of catalytic performance through atomic level control [42]. Fig. S1 shows the executable route to synthesize the electrocatalysts of BAC-COFs by using some commercially available chemical reactants. Actually, many similar electrocatalysts with the bimetallic units anchored on graphene have been experimentally synthesized in several simple steps for electrocatalytic applications [27–33].

The stability of heterogeneous M_1/M_2 -BAC-COFs was determined by calculating the formation energy [43,44] and comparing with the corresponding homogeneous M_1/M_1 -BAC-COFs and M_2/M_2 -BAC-COFs. Many BACs (e.g., Fe/Ni, Fe/Fe, Co/Zn, Fe/Co and Co/Zn) predicted by the formation energy method have been synthesized experimentally, as listed in Table S14. Those BAC-COFs with high formation energy catalysts candidates may be unstable and will be excluded. As shown in Fig. 1b and Table S9, Sc-, Ti-, and V-based BAC-COFs have relatively high formation energy due to their relatively large atomic radius. There are a number of heterogeneous M_1/M_2 BAC-COFs with lower formation energy, which are energetically more favorable than M_1/M_1 and M_2/M_2 , such as Cr/

 M_2 -BAC-COFs, Fe/ M_2 -BAC-COFs. Thus, most of the BAC-COF catalysts could be synthesized from the viewpoint of thermodynamics, except for Sc-, Ti-, and V-based M_1/M_2 -BAC-COFs.

2.2. Electronic structures and catalytic mechanisms of BAC-COFs

Since experimental results show that the reaction of two electron transfer most likely occurs in CO₂RR [27], we here only focus on simple but common products, namely CO and HCOOH. Fig. 1c shows all the possible intermediates and reaction pathways of CO₂RR to form CO and HCOOH products on BAC-COFs. There are four elementary reactions in CO₂RR (Fig. 1c), including: (i) CO₂ adsorption, (ii) CO₂ activation, (iii) chemical formation, and (iv) products desorption. We explored CO₂RR mechanism on different " M_1/M_2-N_6 " structures, starting from the initial step of CO_2 adsorption at the active sites. In the initial step, both metal ions in " $M_1/$ M₂-N₆" catalytic unit favorably provide their empty orbits or electron pairs to satisfy the complex coordination of intermediates into an appropriate state and result in six possible intermediates in CO₂ chemisorption. According to the calculations, most of the BACs can spontaneously chemisorb CO2 molecules with moderate adsorption energy except for Sc/M₂-BACs. The catalytic units with Sc have stronger adsorption ability to capture CO₂, which conforms to the previous literature that the Sc-SAC weaken the bond strength of C-O bonds in CO₂ molecules and enhance the adsorption of their intermediate [45]. On the contrary, most of the corresponding SACs have a relatively higher energy barrier in bonding CO2, which limits their catalytic activity [46].

Thereafter, the first proton begins to approach the *CO₂ intermediates and further forms twelve possible CO₂ activating intermediates after the first hydrogenation reaction. Generally, those CO₂ activating intermediates can be classified into two categories: *COOH and *OCHO, which are critical intermediates for the formation of CO and HCOOH in CO₂RR, respectively [47]. To determine whether CO or HCOOH is the dominant product in CO₂RR, the overpotential (Supporting Information) is employed as an effective criterion to predict the preferential product in the competition reactions [48]. The overpotentials of CO (η^{CO}) and HCOOH (η^{HCOOH}) for BACs were calculated and listed in Tables S6 and S7. Fig. 2a and 2b graphically shows the results—all of the BAC-COFs have a higher overpotential for HCOOH (η^{HCOOH}) than that for CO (η^{CO}), indicating that the formation of HCOOH in the overall conversion of CO₂-RR is unfavorable compared to CO. Hence, HCOOH is inhibited in CO_2RR because there is a huge energy change (ΔG_3) in the formation of *HCOOH intermediate in the third elementary reaction for most of the BAC-COFs (Fig. S2), but the free energy for forming CO at each elementary reaction is closer to the ideal value. Furthermore, HCOOH could not be formed via *COOH intermediates (*COOH → *HCOOH), either, because the second proton attacking the inner C atom of the *COOH intermediate is inadvisable compared to the external O atom (Fig. S3). In principle, the protons (positive) have more tendency to interact with -OH moiety (with negative charge) in *COOH intermediate than C moiety (with positive charge) to form chemical bonds due to electrostatic attraction [49]. This prediction that CO is dominant in two-electron CO₂RR is basically consistent with the experimental results, and also prove that the CO₂RR mechanism with *COCOOH as a critical intermediate in Fe/Ni bimetallic catalytic center, proposed by Zhao [27], is implausible. Therefore, in CO₂RR, the pathway to produce CO $(CO_2 \rightarrow {^*CO_2} \rightarrow {^*COOH} \rightarrow {^*CO} \rightarrow CO)$ involves two elementary reactions of electrochemical hydrogenation and two physical adsorption/desorption reaction without electron transfer [50]. The bimetallic catalytic center in BAC-COFs can provides variable coordination modes to facilitate the formation of up to ten reaction mechanisms for CO products, which is more flexible than most electrocatalysts with single catalytic site [51].

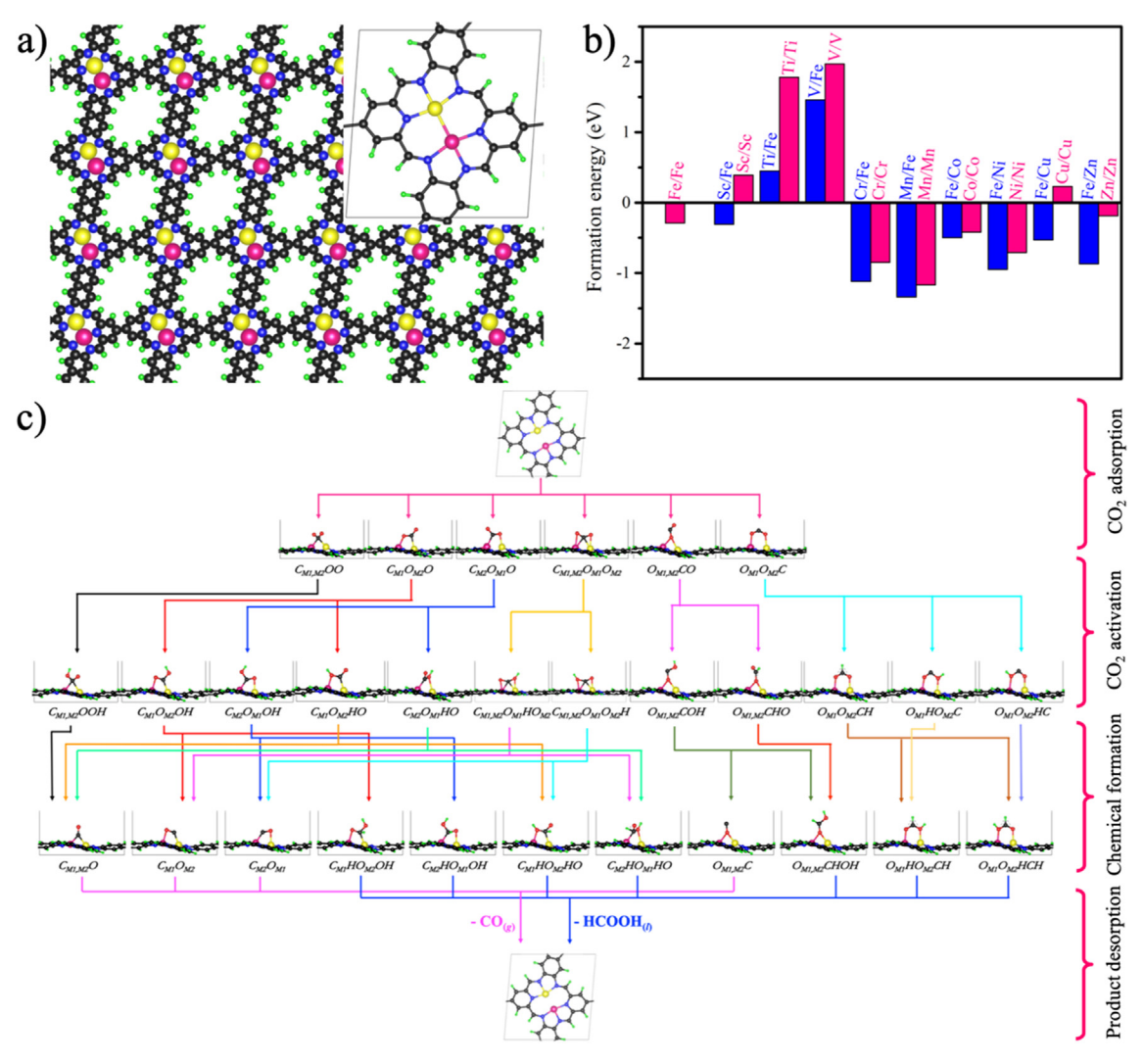


Fig. 1. (a) Schematic of a BAC-based COF structure (the inset in the upper right corner is a " M_1/M_2 - N_6 " catalytic unit). The black, blue, green, yellow and pink colors represent C, N, H, M_1 , and M_2 , respectively; (b) The formation energy of Fe/ M_2 -BAC-COFs, Fe/Fe-BAC-COF and M_2/M_2 -BAC-COF; (c) The possible catalytic mechanisms of two-electron CO₂RR on BACs, including (i) CO₂ chemisorption, (ii) CO₂ activation, (iii) chemical formation, and (iv) product desorption. The proton and electron (H^*+e^-) in the elementary reactions are omitted for simplification. The black, blue, green, yellow, pink, and red colors represent C, N, H, M_1 , M_2 , and O, respectively.

The combination of 3d transition metals can form numerous bimetal catalytic structures, each of which may have different catalytic mechanism and activities, depending on the type of the metals and their synergetic effect. Fig. 2a shows the free energy diagram for typical electrocatalysts of Fe/M2-BACs toward CO products in CO₂RR. Fe/Zn-BAC is theoretically one of the best electrocatalysts among them, with the lowest overpotential ($\eta^{CO} = 0.05$ -V). In contrast, Fe-SAC (η^{CO} = 0.81 V) and Zn-SAC (η^{CO} = 1.42 V) have relatively poor catalytic activity in CO₂RR to form CO [45]. In addition to Fe/Zn-BAC, Fe/Ni-BAC also have relatively higher catalytic activity (η^{CO} = 0.40 V) than corresponding Fe-SAC and Ni-SAC, which was verified by the experimental results that the Fe/ Ni-BAC has lower onset potential and higher Faradaic efficiency [27]. Therefore, the BAC-COFs would effectively reduce the over potential in CO₂RR and demonstrate excellent catalytic performance.

In the prediction of catalytic activities and selectivity of the BACs, HER must be considered because H₂ competes with CO *via* adverse HER due to its low thermodynamic potential close to CO₂-RR [52]. This side reaction was calculated under the same conditions for CO₂RR, and the free energy diagrams for typical Fe/M₂-

BAC-COFs are shown in Fig. 2c. Among those catalysts, Co/Cu-BAC-COFs exhibit the best HER catalytic performance with a negligible energy barrier ($\eta^{\rm H2}$ = 0.05 V) for HER (Fig. S4 and Table S8), even exceeding the noble catalyst of Pt ($\eta^{\rm H2}$ = 0.10 V) [40]. Similarly, the overpotentials ($\eta^{\rm CO}$ vs $\eta^{\rm H2}$) were utilized as an

important reference here to predict the preference of CO₂RR and HER on BAC-COFs. As shown in Fig. 2d, HER-dominated region $(\eta^{CO} > \eta^{H2})$ includes almost all of the Ti-, Cu-based BACs. About half of the BAC-COFs, including most of the Fe-, Ni-, Zn-based BAC-COFs, are located in the CO-dominated regime ($\eta^{CO} < \eta^{H2}$), in which the reactions occur in favor of CO₂RR to CO. However, in predicting the selectivity of the BACs using the overpotential criterion, the value of η^{H2} should be considered as well because a low value of $\eta^{\rm H2}$ implies strong competition from HER. For example, Fe/Zn-BAC has the lowest CO_2RR overpotential ($\eta^{CO} = 0.05 \text{ V}$), but its HER overpotential (η^{H2} = 0.2 V) is very close to that of Pt, the best HER catalyst. Therefore, Fe/Zn-BAC might not be the best catalysts for CO₂RR. In the same CO-dominated regime, Fe/Ni-BAC is predicted to preferentially promote CO2RR while suppressing HER due to its relatively high HER overpotential (η^{H2} = 0.51 V). This prediction is consistent with the experimental results that the CO is

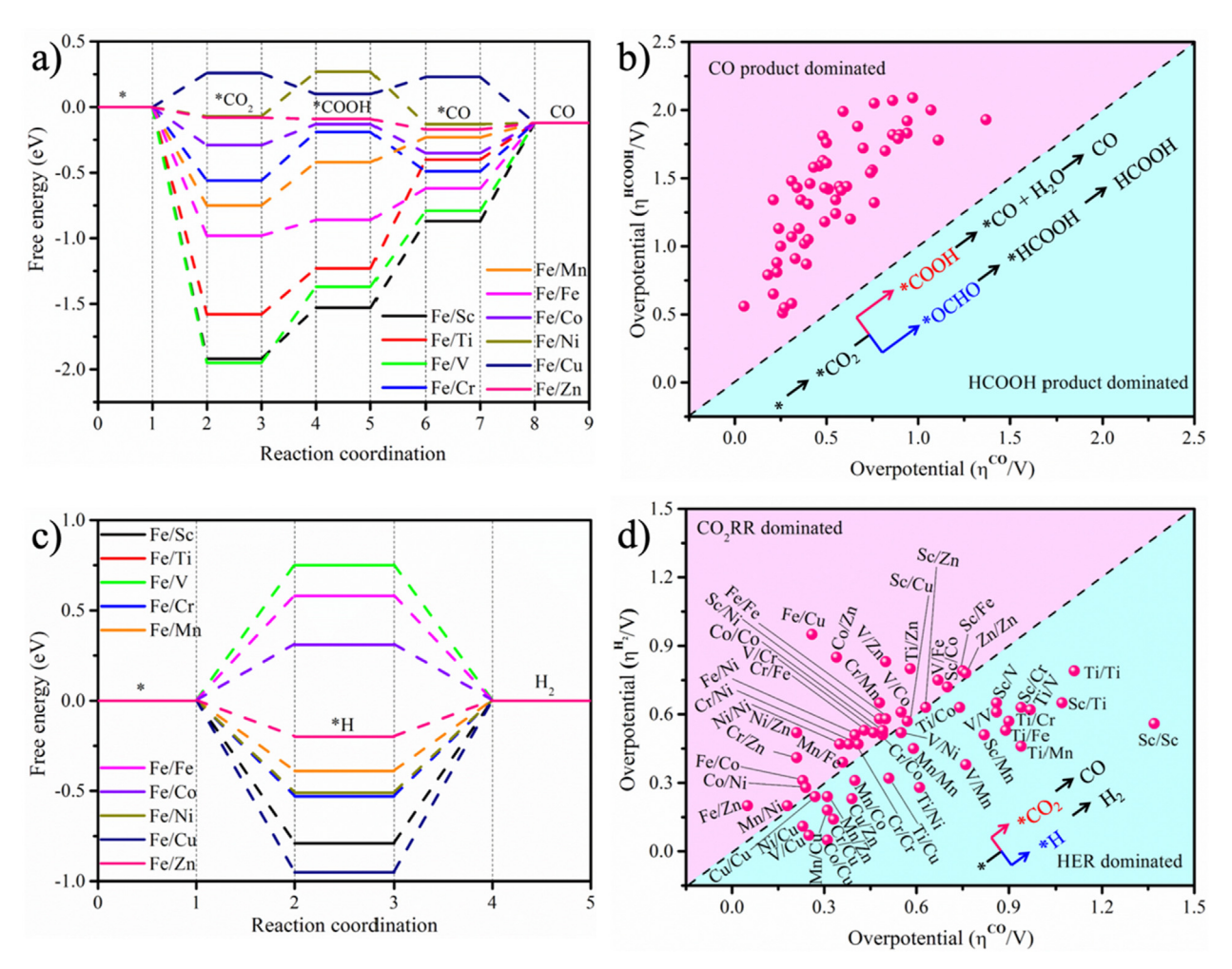


Fig. 2. (a) and (c) Free energy diagrams for typical electrocatalysts of Fe/M₂-BAC-COFs for CO in CO₂RR and H₂ in HER, respectively; (b) and (d) The overpotentials of HCOOH (η^{HCOOH}) or H₂ (η^{H2}) as a function of the overpotential of CO (η^{CO}) on BAC-COFs.

dominant in Fe/Ni-BAC with high Faradaic efficiency (FE% > 90%) [27]. Using the similar rule, Fe/Cu- and Ni/Zn-BACs are identified to be the excellent electrocatalysts with the low overpotential (~0.25 V) while strongly suppressing side reactions (η^{H2} > 0.5 V). Actually, most of BAC-COFs locate near the midline, suggesting that the side main reaction may be accompanied by the side reaction because their overpotentials are very close. Hence, the difference in the overpotential of CO₂RR (η^{CO}) and HER (η^{H2}) could be used as a measure to accurately predict the catalytic selectivity of the catalysts.

2.3. Descriptors and design principles for screening BAC-COFs

It is of interest to develop effective descriptors/design principles that have predictive power and enable to quickly search for the best catalysts from the numerous BAC-COFs. As demonstrated above, overpotential can be used to effectively evaluate the catalytic activity and selectivity. Fig. 3a shows the color-coded diagram of overpotential ($\eta^{\rm CO}$) for all the BAC-COFs (Table S6). Overall, the overpotential tends to decrease with increasing the atomic number of the 3d transition metals. To describe the catalytic activity of the BAC-COFs, we selected the adsorption strength of *COOH and *CO as descriptors since this adsorption strength have an indispensable contribution in determining the CO₂RR catalytic performance [53]. As show in Fig. 3b, a volcano-shaped relationship was formed between the overpotential ($\eta^{\rm CO}$) and bonding

energy of ΔG^*_{COOH} - ΔG^*_{CO} . Obviously, the Fe/Zn-BAC locates at the summit of the volcano and emerges as the best CO₂RR catalytic activity (η^{CO} = 0.05 V) in the BACs. The Sc/M₂-BACs have large overpotential because their extremely strong adsorption capacity hinders the subsequent reaction and the separation of the final product. Thermodynamically, most of the BAC-COFs (η^{CO} < 0.70 V) have higher catalytic activity than the noble metal catalyst of Au [54] (η^{CO} = 0.70 V) and Ag [55] (η^{CO} = 0.86 V) (Table S10). The BAC-COFs are also superior in catalyzing CO₂RR over the widespread SACs, e.g., Co-SACs (0.77 V) and Fe-SACs (0.81 V) [45], as shown in Fig. S6. Therefore, the bonding energy as a descriptor can be used to predict the CO₂RR catalytic performance of different BACs.

However, the bonding energy is not an ideal principle for designing CO₂RR electrocatalysts because it is not directly correlated with the intrinsic properties of the active center of BACs. Here, we have proposed a new descriptor, involving the electronic characteristics (X/electronegativity and W/work function) and geometric configuration (E/cohesive energy), that is, $\Phi = [(X_{M1} + X_{M2})] \times [(W_{M1} + W_{M2})]/[(E_{M1} + E_{M2})]$ (see the details in Supporting Information), and used it to describe the catalytic activity of BACs. Fig. 3c and 3d shows the overpotential (η^{CO}) or (η^{H2}) of BAC-COFs in CO₂RR as a function of the descriptor (Φ). The new descriptor (Φ) works reasonably well to establish volcanos relationship between the overpotential and intrinsic properties for both SACs, and BACs. It seems that the new descriptor also works for Au and

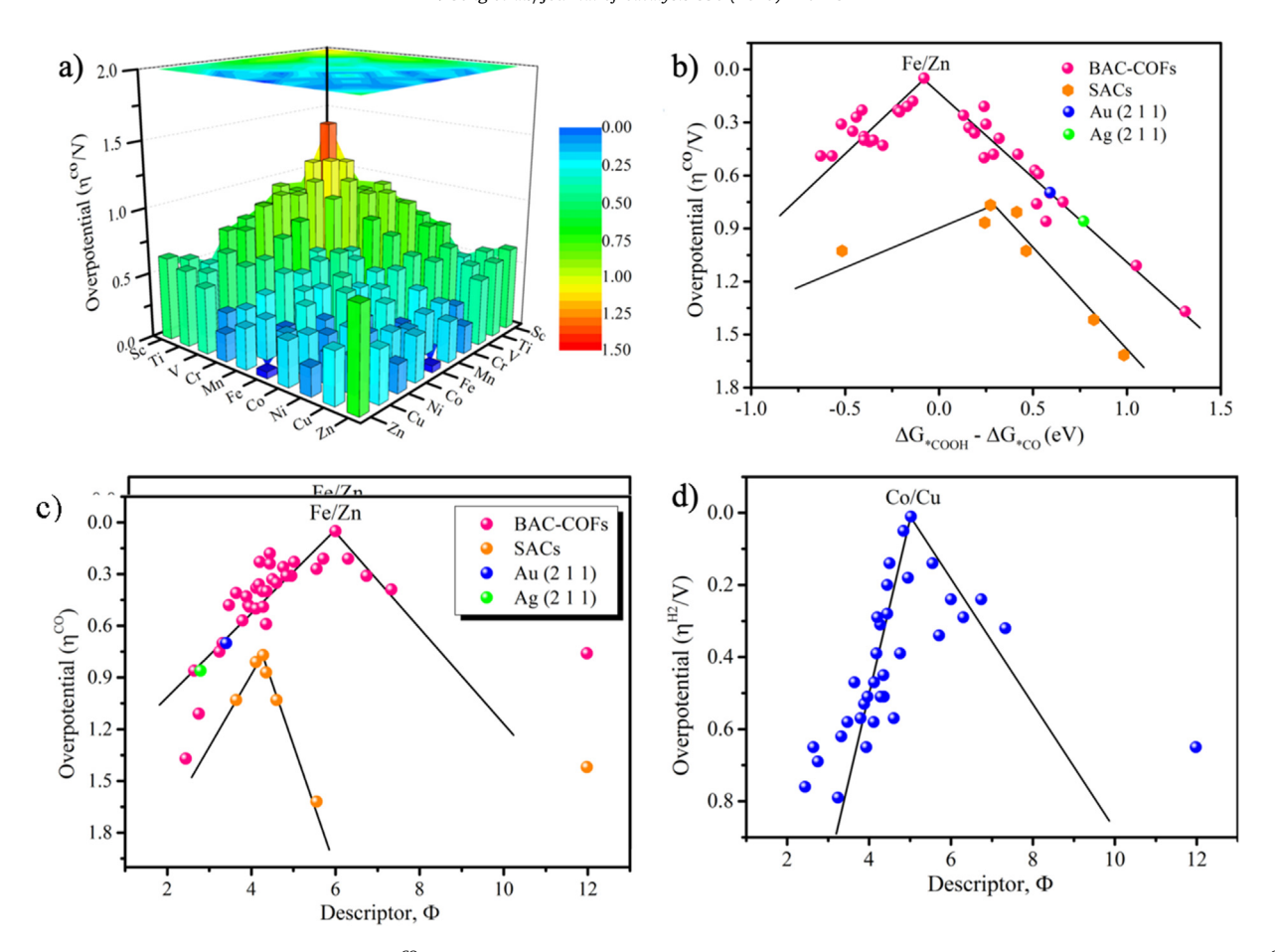


Fig. 3. (a) Color-coded diagram of the overpotential (η^{CO}) for BAC-COFs, the top square is the 2D projected image; (b) The overpotential of CO₂RR to form CO (η^{CO}) as a function of the bonding energy of ΔG^{*}_{COOH} – ΔG^{*}_{CO} , the pink, orange, blue and green are BAC-COFs, SACs, Au (211) and Ag (211), respectively; (c) The overpotential of CO₂RR to form CO (η^{CO}) as a function of the descriptor (Φ); (d) The overpotential of HER to produce H₂ (η^{H2}) as a function of the descriptor (Φ).

Ag catalysts although other metals need to be confirmed. As shown in Fig. 3c, Fe/Zn-BAC has the highest catalytic activity for CO formation in Fe/M₂-BAC-COFs. Moreover, Fe/Co-BAC ($\eta^{CO}=0.23$ V) and Fe/Ni-BAC ($\eta^{CO}=0.40$ V) are located near the summit of the volcano and may also show high performance in CO₂RR. On the other hand, the Sc/M₂-BACs appear at the volcano bottom, shows high overpotential and relatively poor CO₂RR catalytic performance.

The predictive power of the new descriptor stems from its correlation with the inherent properties of bimetal active centers. Fig. 4 shows the binding energy of the intermediates, *CO₂ ($\Delta G_{^*CO2}$), *COOH ($\Delta G_{^*COOH}$) and *CO ($\Delta G_{^*CO}$), as a function of the descriptor (Φ) for Fe/M₂-BAC-COFs. For Φ < 4.0 (e.g. Fe/Sc-BAC),

the catalysts tend to strongly adsorb the intermediates, while those catalysts with $\Phi > 4.2$ (e.g., Fe/Co-BAC and Fe/Zn-BAC) show relatively reasonable binding energy. Thus, the geometric and electronic structures of the active center would be optimized by varying the composition of the bimetal pair. At certain composition, the intermediates could achieve a nearly ideal adsorption or desorption state due to synergetic effect of the bimetals in the active centers, which would significantly enhance the catalytic activity. Therefore, the new descriptor (Φ) is effective to predict the catalytic activities of BAC-COFs for CO₂RR.

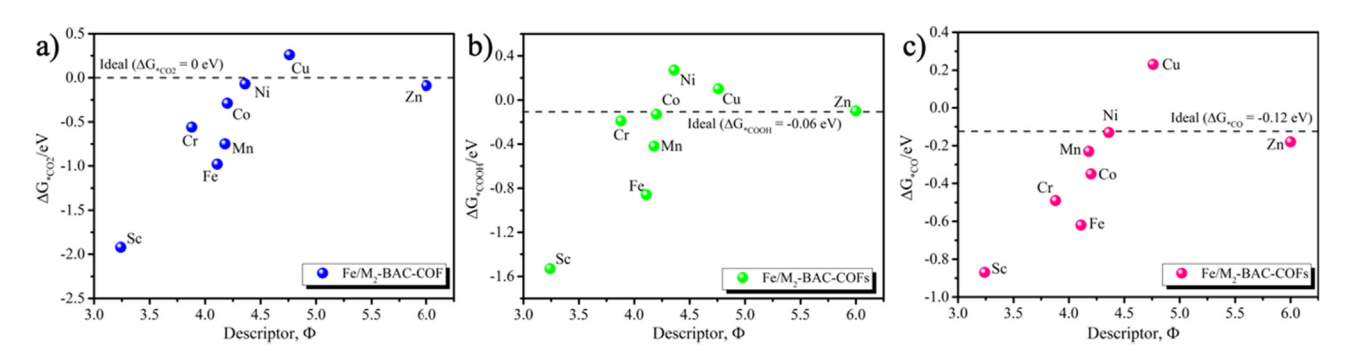


Fig. 4. The binding energy of the critical intermediates in CO_2RR , (a) ΔG_{COO} , (b) ΔG_{COOH} and (c) ΔG_{CO} , as a function of descriptor (Φ).

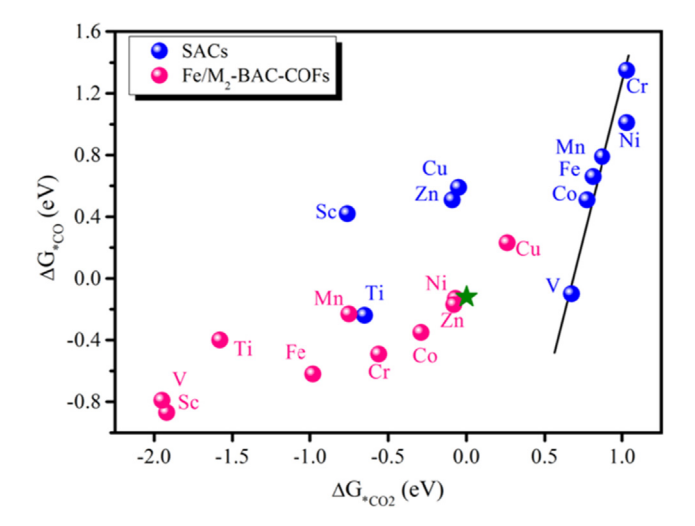


Fig. 5. The relationship between the bonding energy of *CO₂ (ΔG - $_{CO2}$) and *CO (ΔG - $_{CO}$) intermediates on SACs and Fe/M₂-BAC-COFs, the star represents ideal catalysts with zero overpotential (η ^{CO} = 0).

3. Discussion

Our calculations predict that BACs have much lower overpotential, and thus higher catalytic activity and selectivity than SACs, as illustrated in Fig. 3c. This prediction is supported by the experimental results. We have cited the experimental data reported so far for SACs [56] and BACs (Table S14). This demonstrates the pre-

dictive power of the descriptor for guiding the rational design of BACs in highly efficient CO₂ conversion.

Why are the BACs so effective in catalyzing the various chemical reactions in terms of their activity and selectivity? This may be attributed to their ability to weaken or break the scaling relations in the chemical reactions. In fact, catalysts control the rates in chemical reactions by changing the bonding energy of intermediates relative to one another. For SACs as an example, *CO2 intermediate can be readily adsorbed via end-on configuration, in which C in CO₂ forms a bond with the metal ion (i.e., C-M bond). The subsequent intermediates of *COOH, *HCOOH and *CO will inherit this adsorption model to form C-M bond. Since all the intermediates have the same C-M bond. The adsorption strengths exhibit highly correlated behavior between different adsorbates (Fig. 5), known as adsorbate scaling relations; when a catalyst binds one adsorbate more strongly, it tends to bind similar adsorbates more strongly as well [57]. Although the relationships are useful for fast screening for catalyst discovery, the design flexibility in catalysis is largely limited [58,59]. As shown in Fig. 5, the binding energy of CO in the last step of CO₂RR is highly correlated with that of CO₂ in the initial step for SACs except for Sc, Ti, Zn and Cu that have different adsorption modes. This relationship limits the design space of the SACs to improve their catalytic activity.

In the BAC-COFs, there are two metal ions available for adsorption at active centers. The intermediates could form different bonds with the two metal ions. For example, CO₂, COOH, and CO could adsorb on two different metal ions in end-on or side-on mode while C and O could bond with different metals, resulting in a large variety of bonding structures (e.g., C-M1, C-M2, O-M1, O-M2, etc.). Compared with SACs that have only two adsorption

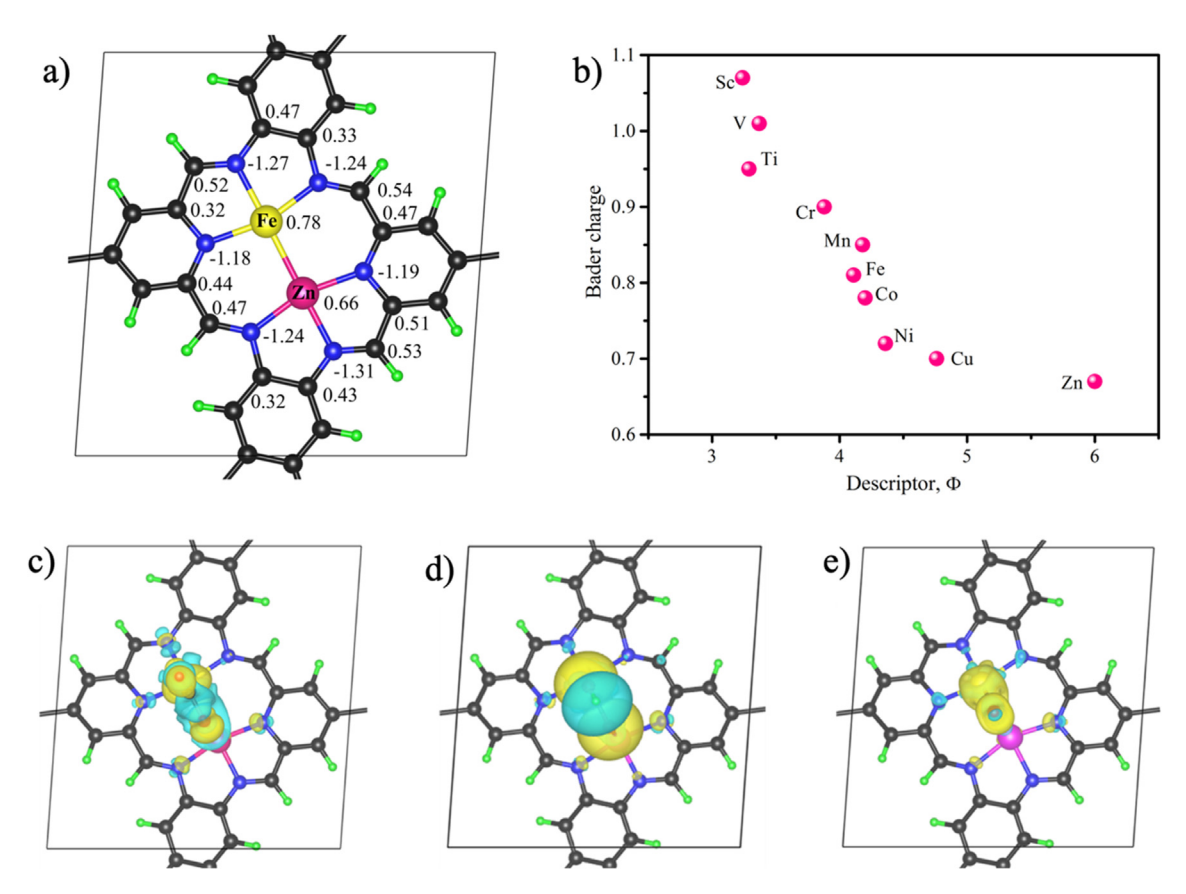


Fig. 6. (a) The Bader charge on Fe/Zn-BAC-COFs, the black, blue, green, yellow and pink color balls represent C, N, H, Fe, Zn, respectively; (b) The Bader charge as a function of descriptor (Φ) for typical electrocatalysts of Fe/M₂-BAC-COFs; (c-e) The charge transfer distribution on Fe/Zn-BAC/COFs with critical intermediates of *CO₂, *COOH and *CO. The blue and yellow colors indicate the positive and negative values of electron quantities, respectively. The isosurface value is set to 0.0036 e/Bohr³.

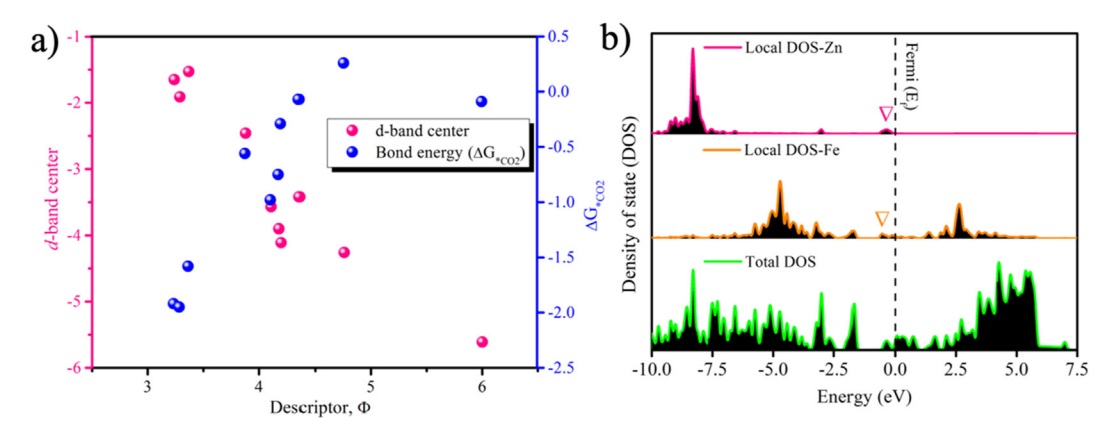


Fig. 7. (a) The *d*-band center (ε_d , pink) and binding energy of CO₂ (ΔG_{CO2} , blue) as a function of descriptor (Φ) for typical electrocatalysts of Fe/M₂-BACs/COFs; (b) The density of state of Fe/Zn-BAC-COF. The green, orange and pink lines represent total density of states (TDOS), local density of states (LDOS) of Fe and Zn, respectively.

modes [45], there are nine reaction mechanisms for BACs toward CO (Fig. 1c), which facilitate intermediates to achieve the ideal state and thus improve the catalytic activity of CO_2RR . Therefore, the scaling relationship between the energy of these intermediate adsorbents is significantly weaken or broken in BAC-COFs due to the different adsorption modes between CO_2 and CO, as shown in Fig. 5. In addition, the bimetal catalytic sites provide flexible coordination environments of intermediates in the reaction to optimize the adsorption energy of individual intermediates.

The intrinsic descriptor (Φ) that we proposed performs well in establishing volcano relationships associated with the overpotentials (η^{CO}), a measure of catalytic activities, from which the desirable catalysts are expediently predicted. This provides an effective design principle for guiding the experiments to synthesize the electrocatalysts with high catalytic activity and product selectivity. To reveal the catalytic mechanism and explain the superior catalytic activity of BACs, we further simulated the charge redistribution on BAC-COFs. Figs. 6a and S8 show the charge distributions on Fe/M₂-BAC-COFs with positive charge on metals ($\pm 0.6e$ to $\pm 1.1e$), and negative charge on nitrogen (-1.2e to -1.3e). The values of Bader charge of Fe/M2-BAC-COFs are listed in Table S12. The amount of charges on metals is approximately linearly proportional to the descriptor (Φ) (Fig. 6b). Hence, the descriptor (Φ) is closely related to the charge state of metal centers. The charges on metals will strongly affect the bonding strength of intermediates on CO₂RR (Fig. S7). For example, for Fe/Sc, the bonding energy of * CO_2 intermediate (ΔG_1) is too strong for the metal ions with relatively high positive charge, as shown in Fig. 6c-e. The overstrong bonding on intermediates will hinder the further reactions and the product desorption, which results in a large overpotential (η^{CO}) , and consequently poor catalytic activity. As the amount of the positive charge decreases (e.g., Fe/Co, Fe/Zn), the bonding gradually weakens and finally reaches the ideal state, which leads to the enhanced catalytic performance.

The density of state (DOS) of BAC-COFs was also analyzed to explore more details about the $\mathrm{CO}_2\mathrm{RR}$ catalytic performance. It is well known that the electronic states of the metal atoms will split into two-hybrid energy levels, including bonding orbital or antibonding orbital, the former being the electronic state normally occupied under the Fermi level and the latter being occupied above the Fermi Level [60]. According to previous reports [40], the lower the *d*-band center (ϵ_d) position of the electrocatalysts, the higher the occupancy of the anti-bonding state will occur, which weakens the adsorption strength between the adsorbed and electrocatalyst surface. Fig. 7a shows the *d*-band center and binding energy as a function of the descriptor. For Fe/Sc- and Fe/Ti-BACs, there is a rel-

atively high *d*-band center (ϵ_d) (Table S13), indicating that most of electronic states are likely to be distributed in the bonding orbitals, causing a stronger bonding energy of the intermediates. In contrast, Fe/Ni-, Fe/Cu-, Fe/Zn-BACs have a relatively low *d*-band center (ϵ_d), and more electronic states are distributed in anti-bonding orbitals, which reduces the binding energy. Thus, the Fe/Co, and Fe/Zn-BACs have relatively highly CO₂ catalytic performance. Moreover, the density of state (DOS) and local density of state (LDOS) of BAC-COFs provide some complementary details about the catalytic activity. Figs. 7b and S9 show the TDOS and LDOS of Fe/M₂-BAC-COFs and other BAC-COFs, respectively. Among the BAC-COFs, the LDOS peaks of the metals in Fe/Zn-BACs approach to the Fermi level (Fig. 7b), making it easy for electrons to donate to CO₂ and intermediates and consequently the catalyst exhibits a highly CO₂ catalytic performance.

4. Conclusion

In summary, we have designed a class of bimetallic-atoms electrocatalysts with highly catalytic performance for CO₂RR. The CORR reaction pathways, free energy, overpotential, and other related properties were calculated with the DFT methods. A new intrinsic descriptor was proposed to establish the volcano-shaped relationships correlating the bimetal active centers with the catalytic activities, from which the best catalytic performance of the catalysts can be predicted. Fe/Cu-and Ni/Zn-BAC-COFs could be among excellent BAC-COF electrocatalysts with the low overpotential (~0.25V) while suppressing HER side reactions. Most of BAC-COFs have a higher catalytic activity than noble metals electrocatalysts (e.g., Au and Ag), and also exceeding SACs (e.g., Fe-SAC, Co-SAC). This prediction is consistent with the experimental results that Fe/Ni-BAC anchored on graphene shows a lower onset potential and higher Faraday efficiency for CO₂RR than corresponding Fe-SACs and Ni-SACs [27]. The bimetallic catalytic sites can break the limitations of scaling relation to significantly improve the catalytic activity. It is expected that this class of electrocatalysts with bimetallic catalytic sites will provide a new route for discovering high-performance electrocatalysts for energy conversion, and the descriptor proposed in this work will enrich the design principles for guiding the rational design of electrocatalysts for boarder applications.

5. Computation methods

A series of models were developed to simulate CO_2 conversion on BACs with " M_1/M_2 - N_6 " units containing 3d transition metals

 $(M_1 \text{ and } M_2 = Sc, Ti, V, Cr, Mn, Fe, Co, Ni, Cu, and Zn)$. The DFT calculations were performed by using the Vienna Ab initio Simulation Package (VASP) code [61,62] with the Hubbard U (DFT + U) corrections [36] (Table S1). The project-augmented wave generalized gradient approximation (PAW-GGA) pseudopotentials were adopted to describe the electron-ion interaction, and the Perdew-Burke-Ernzerhof (GGA-PBE) functional was utilized to calculate the exchange-correlation energy [63,64]. Spin-polarization was considered in all calculations. Wave functions were expanded using a plane-wave basis set with kinetic energy cutoff of 550 eV and the geometries were fully relaxed until the residual force convergence value on each atom being less 0.01 eV/Å. The Brillouin zone was sampled by $3 \times 3 \times 1$ Gamma k-point mesh for structural optimization and $5 \times 5 \times 1$ for calculation of the density of state (DOS). A vacuum spacing of at least 20 Å in z-direction perpendicular was employed to avert the artificial interactions between the periodically repeated images. The above parameters have been optimized until the energy change is negligible. The free energies are converted from the calculated energies by adding appropriate corrections. More details about computational methods, bonding energy and related parameters are described in Supporting

For commercial noble electrocatalysts of Ag (211), and Au (211) were also calculated their catalytic activity of CO₂RR. We used a p (4 \times 4) unit cell of Ag (211), and Au (211). All of them have four layers in their slab. Geometric optimizations for those noble electrocatalysts were performed by using 3 \times 3 \times 1 Gamma k-point mesh.

Declaration of Competing Interest

The authors declare that they have no known competing financial interests or personal relationships that could have appeared to influence the work reported in this paper.

Acknowledgement

LL, LG, DZ, YS, ZJ, XH and LZ thank the National Key Research and Development Program of China (2017YFA0206500), National Natural Science Foundation of China (51732002, 51973174), Distinguished Scientist Program at BUCT (buctylkxj02), the Fundamental Research Funds for the Central Universities (buctrc202008, 3102019ZD0402), China Scholarships Council (No.201806880044), and US National Science Foundation (1561886 and 1662288) for the support of this research.

Author contributions

Z.X. and L.G. conceived and designed the research. L.G., and D.Z. performed modelling and simulation, L.G. and Z.X. wrote the manuscript. All authors discussed the results and commented on the manuscript.

Appendix A. Supplementary material

Supplementary data to this article can be found online at https://doi.org/10.1016/j.jcat.2020.07.021.

References

 H.A. Hansen, J.B. Varley, A.A. Peterson, J.K. Nørskov, Understanding trends in the electrocatalytic activity of metals and enzymes for CO₂ reduction to CO, J. Phys. Chem. Lett. 4 (3) (2013) 388–392.

- [2] N. Kornienko, Y. Zhao, C.S. Kley, C. Zhu, D. Kim, S. Lin, C.J. Chang, O.M. Yaghi, P. Yang, Metal-organic frameworks for electrocatalytic reduction of carbon dioxide, J. Am. Chem. Soc. 137 (44) (2015) 14129–14135.
- [3] K.P. Kuhl, E.R. Cave, D.N. Abram, T.F. Jaramillo, New insights into the electrochemical reduction of carbon dioxide on metallic copper surfaces, Energy Environ. Sci. 5 (5) (2012) 7050–7059.
- [4] M. Ma, K. Djanashvili, W.A. Smith, Controllable hydrocarbon formation from the electrochemical reduction of CO₂ over Cu nanowire arrays, Angew. Chem. 128 (23) (2016) 6792–6796.
- [5] L.L. Gong, W.T. Yao, Z.Q. Liu, A.M. Zheng, J.Q. Li, X.F. Feng, L.F. Ma, C.S. Yan, M.B. Luo, F. Luo, Photoswitching storage of guest molecules in metal-organic framework for photoswitchable catalysis: exceptional product, ultrahigh photocontrol, and photomodulated size selectivity, J. Mater. Chem. A 5 (17) (2017) 7961–7967.
- [6] S. Lin, C.S. Diercks, Y.-B. Zhang, N. Kornienko, E.M. Nichols, Y. Zhao, A.R. Paris, D. Kim, P. Yang, O.M. Yaghi, C.J. Chang, Covalent organic frameworks comprising cobalt porphyrins for catalytic CO₂ reduction in water, Science 349 (6253) (2015) 1208–1213.
- [7] V. Tripkovic, M. Vanin, M. Karamad, M.E. Björketun, K.W. Jacobsen, K.S. Thygesen, J. Rossmeisl, Electrochemical CO₂ and CO reduction on metal-functionalized porphyrin-like graphene, J. Phys. Chem. C 117 (18) (2013) 9187–9195
- [8] L. Zhang, C.-Y. Lin, D. Zhang, L. Gong, Y. Zhu, Z. Zhao, Q. Xu, H. Li, Z. Xia, Guiding principles for designing highly efficient metal-free carbon catalysts, Adv. Mater. 31 (13) (2019) 1805252.
- [9] T. Zheng, K. Jiáng, N. Ta, Y. Hu, J. Zeng, J. Liu, H. Wang, Large-scale and highly selective CO₂ electrocatalytic reduction on nickel single-atom catalyst, Joule 3 (1) (2019) 265–278.
- [10] I. Azcarate, C. Costentin, M. Robert, J.-M. Savéant, Through-space charge interaction substituent effects in molecular catalysis leading to the design of the most efficient catalyst of CO₂-to-CO electrochemical conversion, J. Am. Chem. Soc. 138 (51) (2016) 16639–16644.
- [11] C.S. Diercks, S. Lin, N. Kornienko, E.A. Kapustin, E.M. Nichols, C. Zhu, Y. Zhao, C. J. Chang, O.M. Yaghi, Reticular electronic tuning of porphyrin active sites in covalent organic frameworks for electrocatalytic carbon dioxide reduction, J. Am. Chem. Soc. 140 (3) (2018) 1116–1122.
- [12] W. Ju, A. Bagger, G.-P. Hao, A.S. Varela, I. Sinev, V. Bon, B.R. Cuenya, S. Kaskel, J. Rossmeisl, P. Strasser, Understanding activity and selectivity of metal-nitrogen-doped carbon catalysts for electrochemical reduction of CO₂, Nat. Commun. 8 (1) (2017) 944.
- [13] C. Costentin, S. Drouet, M. Robert, J.-M. Savéant, A local proton source enhances CO₂ electroreduction to CO by a molecular Fe catalyst, Science 338 (6103) (2012) 90–94.
- [14] J. Bonín, A. Maurin, M. Robert, Molecular catalysis of the electrochemical and photochemical reduction of CO₂ with Fe and Co metal-based complexes. Recent advances, Coordin. Chem. Rev. 334 (2017) 184–198.
- [15] Z. Zhang, J. Xiao, X.-J. Chen, S. Yu, L. Yu, R. Si, Y. Wang, S. Wang, X. Meng, Y. Wang, Z.-Q. Tian, D. Deng, Reaction mechanisms of well-defined metal-N4 sites in electrocatalytic CO₂ reduction, Angew. Chem. Int. Ed. 57 (50) (2018) 16339–16342.
- [16] Y.-R. Wang, Q. Huang, C.-T. He, Y. Chen, J. Liu, F.-C. Shen, Y.-Q. Lan, Oriented electron transmission in polyoxometalate-metalloporphyrin organic framework for highly selective electroreduction of CO₂, Nat. Commun. 9 (1) (2018) 4466.
- [17] P. Su, K. Iwase, T. Harada, K. Kamiya, S. Nakanishi, Covalent triazine framework modified with coordinatively-unsaturated Co or Ni atoms for CO₂ electrochemical reduction, Chem. Sci. 9 (16) (2018) 3941–3947.
- [18] C. Yan, H. Li, Y. Ye, H. Wu, F. Cai, R. Si, J. Xiao, S. Miao, S. Xie, F. Yang, Y. Li, G. Wang, X. Bao, Coordinatively unsaturated nickel-nitrogen sites towards selective and high-rate CO₂ electroreduction, Energy Environ. Sci. 11 (5) (2018) 1204-1210.
- [19] Y. Ouyang, L. Shi, X. Bai, Q. Li, J. Wang, Breaking scaling relations for efficient CO₂ electrochemical reduction through dual-atom catalysts, Chem. Sci. 11 (7) (2020) 1807–1813.
- [20] J. Jiao, R. Lin, S. Liu, W.-C. Cheong, C. Zhang, Z. Chen, Y. Pan, J. Tang, K. Wu, S.-F. Hung, H.M. Chen, L. Zheng, Q. Lu, X. Yang, B. Xu, H. Xiao, J. Li, D. Wang, Q. Peng, C. Chen, Y. Li, Copper atom-pair catalyst anchored on alloy nanowires for selective and efficient electrochemical reduction of CO₂, Nat. Chem. 11 (3) (2019) 222–228
- [21] J.P. Collman, S. Ghosh, A. Dey, R.A. Decréau, Y. Yang, Catalytic reduction of O_2 by cytochrome c using a synthetic model of cytochrome c oxidase, J. Am. Chem. Soc. 131 (14) (2009) 5034–5035.
- [22] A. Bhagi-Damodaran, M.A. Michael, Q. Zhu, J. Reed, B.A. Sandoval, E.N. Mirts, S. Chakraborty, P. Moënne-Loccoz, Y. Zhang, Y. Lu, Why copper is preferred over iron for oxygen activation and reduction in haem-copper oxidases, Nat. Chem. 9 (2016) 257–263.
- [23] M. Xiao, H. Zhang, Y. Chen, J. Zhu, L. Gao, Z. Jin, J. Ge, Z. Jiang, S. Chen, C. Liu, W. Xing, Identification of binuclear Co₂N₅ active sites for oxygen reduction reaction with more than one magnitude higher activity than single atom CoN₄ site, Nano Energy 46 (2018) 396–403.
- [24] P. Zhou, X. Hou, Y. Chao, W. Yang, W. Zhang, Z. Mu, J. Lai, F. Lv, K. Yang, Y. Liu, J. Li, J. Ma, J. Luo, S. Guo, Synergetic interaction between neighboring platinum and ruthenium monomers boosts CO oxidation, Chem. Sci. 10 (23) (2019) 5898–5905.

- [25] F. Li, X. Liu, Z. Chen, 1 + 1' > 2: Heteronuclear biatom catalyst outperforms its homonuclear counterparts for CO oxidation, Small Methods 3 (9) (2019) 1800480
- [26] Y. Li, H. Su, S.H. Chan, Q. Sun, CO₂ electroreduction performance of transition metal dimers supported on graphene: a theoretical study, ACS Catal. 5 (11) (2015) 6658–6664.
- [27] W. Ren, X. Tan, W. Yang, C. Jia, S. Xu, K. Wang, S.C. Smith, C. Zhao, Isolated diatomic Ni-Fe metal-nitrogen sites for synergistic electroreduction of CO₂, Angew. Chem. Int. Ed. 58 (21) (2019) 6972–6976.
- [28] J. Wang, Z. Huang, W. Liu, C. Chang, H. Tang, Z. Li, W. Chen, C. Jia, T. Yao, S. Wei, Y. Wu, Y. Li, Design of N-coordinated dual-metal sites: a stable and active Ptfree catalyst for acidic oxygen reduction reaction, J. Am. Chem. Soc. 139 (48) (2017) 17281–17284.
- [29] Ž. Lu, B. Wang, Y. Hu, W. Liu, Y. Zhao, R. Yang, Z. Li, J. Luo, B. Chi, Z. Jiang, M. Li, S. Mu, S. Liao, J. Zhang, X. Sun, An isolated zinc-cobalt atomic pair for highly active and durable oxygen reduction, Angew. Chem. Int. Ed. 58 (9) (2019) 2622–2626.
- [30] Z.W. Chen, J.-M. Yan, Q. Jiang, Single or double: which is the altar of atomic catalysts for nitrogen reduction reaction?, Small Methods 3 (6) (2019) 1800291.
- [31] W. Ye, S. Chen, Y. Lin, L. Yang, S. Chen, X. Zheng, Z. Qi, C. Wang, R. Long, M. Chen, J. Zhu, P. Gao, L. Song, J. Jiang, Y. Xiong, Precisely tuning the number of Fe atoms in clusters on N-doped carbon toward acidic oxygen reduction reaction, Chem 5 (11) (2019) 2865–2878.
- [32] L. Bai, C.-S. Hsu, D.T.L. Alexander, H.M. Chen, X. Hu, A cobalt-iron double-atom catalyst for the oxygen evolution reaction, J. Am. Chem. Soc. 141 (36) (2019) 14190–14199.
- [33] G. Zhang, Y. Jia, C. Zhang, X. Xiong, K. Sun, R. Chen, W. Chen, Y. Kuang, L. Zheng, H. Tang, W. Liu, J. Liu, X. Sun, W.-F. Lin, H. Dai, A general route via formamide condensation to prepare atomically dispersed metal-nitrogen-carbon electrocatalysts for energy technologies, Energy Environ. Sci. 12 (4) (2019) 1317–1325.
- [34] L. Zhang, Z. Xia, Mechanisms of oxygen reduction reaction on nitrogen-doped graphene for fuel cells, J. Phys. Chem. C 115 (22) (2011) 11170–11176.
- [35] M. Karamad, H.A. Hansen, J. Rossmeisl, J.K. Nørskov, Mechanistic pathway in the electrochemical reduction of CO₂ on RuO₂, ACS Catal. 5 (7) (2015) 4075– 4081.
- [36] C.-Y. Lin, L. Zhang, Z. Zhao, Z. Xia, Design principles for covalent organic frameworks as efficient electrocatalysts in clean energy conversion and green oxidizer production, Adv. Mater. 29 (17) (2017) 1606635.
- [37] Z. Zhao, M. Li, L. Zhang, L. Dai, Z. Xia, Design principles for heteroatom-doped carbon nanomaterials as highly efficient catalysts for fuel cells and metal-air batteries, Adv. Mater. 27 (43) (2015) 6834–6840.
- [38] B. Hammer, J.K. Norskov, Why gold is the noblest of all the metals, Nature 376 (6537) (1995) 238–240.
- [39] J. Suntivich, H.A. Gasteiger, N. Yabuuchi, H. Nakanishi, J.B. Goodenough, Y. Shao-Horn, Design principles for oxygen-reduction activity on perovskite oxide catalysts for fuel cells and metal-air batteries, Nat. Chem. 3 (7) (2011) 546-550.
- [40] H. Xu, D. Cheng, D. Cao, X.C. Zeng, A universal principle for a rational design of single-atom electrocatalysts, Nat. Catal. 1 (5) (2018) 339–348.
- [41] Y. Liu, J. Wu, K.P. Hackenberg, J. Zhang, Y.M. Wang, Y. Yang, K. Keyshar, J. Gu, T. Ogitsu, R. Vajtai, J. Lou, P.M. Ajayan, B.C. Wood, B.I. Yakobson, Self-optimizing, highly surface-active layered metal dichalcogenide catalysts for hydrogen evolution, Nat. Energy 2 (9) (2017) 17127.
- [42] M.-X. Wu, Y.-W. Yang, Applications of covalent organic frameworks (COFs): From gas storage and separation to drug delivery Chin, Chem. Lett. 28 (6) (2017) 1135–1143.
- [43] Y. Yanga, H. Zhang, Z. Liang, Y. Yin, B. Mei, F. Song, F. Sun, S. Gu, Z. Jiang, Y. Wu, Z. Zhu, Role of local coordination in bimetallic sites for oxygen reduction: A theoretical analysis, J. Energy Chem. 44 (2020) 131–137.
- [44] X. Guo, J. Gu, S. Lin, S. Zhang, Z. Chen, S. Huang, Tackling the activity and selectivity challenges of electrocatalysts toward the nitrogen reduction

- reaction via atomically dispersed biatom catalysts, J. Am. Chem. Soc. 142 (12) (2020) 5709–5721.
- [45] L. Gong, D. Zhang, C.Y. Lin, Y. Zhu, Y. Shen, J. Zhang, X. Han, L. Zhang, Z. Xia, Catalytic mechanisms and design principles for single-atom catalysts in highly efficient CO₂ conversion, Adv. Energy Mater. 9 (44) (2019) 1902625.
- [46] Z. Wang, J. Zhao, Q. Cai, CO₂ electroreduction performance of a single transition metal atom supported on porphyrin-like graphene: a computational study, Phys. Chem. Chem. Phys. 19 (34) (2017) 23113–23121.
- [47] Z. Zhao, G. Lu, Computational screening of near-surface alloys for CO₂ electroreduction, ACS Catal. 8 (5) (2018) 3885–3894.
- [48] M. Karamad, V. Tripkovic, J. Rossmeisl, Intermetallic alloys as CO electroreduction catalysts—role of isolated active sites, ACS Catal. 4 (7) (2014) 2268–2273.
- [49] F. Calle-Vallejo, J.I. Martínez, J. Rossmeisl, Density functional studies of functionalized graphitic materials with late transition metals for oxygen reduction reactions, Phys. Chem. Chem. Phys. 13 (34) (2011) 15639–15643.
- [50] K. Jiang, S. Siahrostami, A.J. Akey, Y. Li, Z. Lu, J. Lattimer, Y. Hu, C. Stokes, M. Gangishetty, G. Chen, Y. Zhou, W. Hill, W.-B. Cai, D. Bell, K. Chan, J.K. Nørskov, Y. Cui, H. Wang, Transition-metal single atoms in a graphene shell as active centers for highly efficient artificial photosynthesis, Chem 3 (6) (2017) 950-960
- [51] M.-J. Cheng, Y. Kwon, M. Head-Gordon, A.T. Bell, Tailoring metal-porphyrinlike active sites on graphene to improve the efficiency and selectivity of electrochemical CO₂ reduction, J. Phys. Chem. C 119 (37) (2015) 21345–21352.
- [52] W. Zhang, Y. Hu, L. Ma, G. Zhu, Y. Wang, X. Xue, R. Chen, S. Yang, Z. Jin, Progress and perspective of electrocatalytic CO₂ reduction for renewable carbonaceous fuels and chemicals, Adv. Sci. 5 (1) (2018) 1700275.
- [53] A.A. Peterson, F. Abild-Pedersen, F. Studt, J. Rossmeisl, J.K. Nørskov, How copper catalyzes the electroreduction of carbon dioxide into hydrocarbon fuels, Energy Environ. Sci. 3 (9) (2010) 1311–1315.
- [54] W. Zhu, R. Michalsky, Ö. Metin, H. Lv, S. Guo, C.J. Wright, X. Sun, A.A. Peterson, S. Sun, Monodisperse Au nanoparticles for selective electrocatalytic reduction of CO₂ to CO, J. Am. Chem. Soc. 135 (45) (2013) 16833–16836.
- [55] M.R. Singh, J.D. Goodpaster, A.Z. Weber, M. Head-Gordon, A.T. Bell, Mechanistic insights into electrochemical reduction of CO₂ over Ag using density functional theory and transport models, Proc. Natl. Acad. Sci. U.S.A. 114 (42) (2017) E8812–E8821.
- [56] F. Pan, W. Deng, C. Justiniano, Y. Li, Identification of champion transition metals centers in metal and nitrogen-codoped carbon catalysts for CO₂ reduction, Appl. Catal. B 226 (2018) 463–472.
- [57] F. Abild-Pedersen, J. Greeley, F. Studt, J. Rossmeisl, T.R. Munter, P.G. Moses, E. Skúlason, T. Bligaard, J.K. Nørskov, Scaling properties of adsorption energies for hydrogen-containing molecules on transition-metal surfaces, Phys. Rev. Lett. 99 (1) (2007), 016105.
- [58] J. Greeley, Theoretical heterogeneous catalysis: scaling relationships and computational catalyst design, Annu. Rev. Chem. Biomol. 7 (1) (2016) 605– 635
- [59] A. Khorshidi, J. Violet, J. Hashemi, A.A. Peterson, How strain can break the scaling relations of catalysis, Nat. Catal. 1 (4) (2018) 263–268.
- [60] S. Liu, Z. Li, C. Wang, W. Tao, M. Huang, M. Zuo, Y. Yang, K. Yang, L. Zhang, S. Chen, P. Xu, Q. Chen, Turning main-group element magnesium into a highly active electrocatalyst for oxygen reduction reaction, Nat. Commun. 11 (1) (2020) 938.
- [61] P. Hirunsit, Electroreduction of carbon dioxide to methane on copper, coppersilver, and copper-gold catalysts: A DFT study, J. Phys. Chem. C 117 (16) (2013) 8262–8268.
- [62] L.C. Grabow, M. Mavrikakis, Mechanism of methanol synthesis on Cu through CO₂ and CO hydrogenation, ACS Catal. 1 (4) (2011) 365–384.
- [63] I.V. Solovyev, P.H. Dederichs, V.I. Anisimov, Corrected atomic limit in the local-density approximation and the electronic structure of d impurities in Rb, Phys. Rev. B 50 (23) (1994) 16861–16871.
- [64] J.P. Perdew, K. Burke, M. Ernzerhof, Generalized Gradient approximation made simple, Phys. Rev. Lett. 77 (18) (1996) 3865–3868.